ORNL/SPR-2020/1582

Engineering scale molten salt corrosion and chemistry code development

A Graham
RR Pillai
BS Collins
JW McMurray

July 31, 2020

OAK RIDGE NATIONAL LABORATORY
MANAGED BY UT-BATTELLE FOR THE US DEPARTMENT OF ENERGY

DOCUMENT AVAILABILITY

Reports produced after January 1, 1996, are generally available free via US Department of Energy (DOE) SciTech Connect.

Website www.osti.gov

Reports produced before January 1, 1996, may be purchased by members of the public from the following source:

National Technical Information Service
5285 Port Royal Road
Springfield, VA 22161
Telephone 703-605-6000 (1-800-553-6847)
TDD 703-487-4639
Fax 703-605-6900
E-mail info@ntis.gov
Website http://classic.ntis.gov/

Reports are available to DOE employees, DOE contractors, Energy Technology Data Exchange representatives, and International Nuclear Information System representatives from the following source:

Office of Scientific and Technical Information
PO Box 62
Oak Ridge, TN 37831
Telephone 865-576-8401
Fax 865-576-5728
E-mail reports@osti.gov
Website http://www.osti.gov/contact.html

This report was prepared as an account of work sponsored by an agency of the United States Government. Neither the United States Government nor any agency thereof, nor any of their employees, makes any warranty, express or implied, or assumes any legal liability or responsibility for the accuracy, completeness, or usefulness of any information, apparatus, product, or process disclosed, or represents that its use would not infringe privately owned rights. Reference herein to any specific commercial product, process, or service by trade name, trademark, manufacturer, or otherwise, does not necessarily constitute or imply its endorsement, recommendation, or favoring by the United States Government or any agency thereof. The views and opinions of authors expressed herein do not necessarily state or reflect those of the United States Government or any agency thereof.

ORNL/SPR-2020/1582

Department of Energy Office of Nuclear Energy
Nuclear Energy Advanced Modeling and Simulation Program

ENGINEERING SCALE MOLTEN SALT CORROSION AND CHEMISTRY CODE DEVELOPMENT

A Graham
RR Pillai
BS Collins
JW McMurray

Date Published:
July 31, 2020

Prepared by
OAK RIDGE NATIONAL LABORATORY
Oak Ridge, TN 37831-6283
managed by
UT-BATTELLE, LLC
for the
US DEPARTMENT OF ENERGY
under contract DE-AC05-00OR22725

CONTENTS

ABSTRACT

A new engineering scale transport code Mole is described. Mole was developed using the Multiphysics Object-Oriented Simulation Environment (MOOSE) framework for solving species transport problems in flowing liquid. It is applied to leaching of Cr from alloys into molten salts part a of a multi-physics, multi-scale approach for coupling chemistry with mechanical behavior modeling. Demonstrations of the leaching phenomenon were benchmarked to experimental data provided by the Molten Salt Reactor campaign and the results are presented.

1. STRUCTURAL MATERIALS AND CHEMISTRY CURRENT AND LONG-RANGE GOALS: A CHEMISTRY PERSPECTIVE

The Nuclear Energy Advanced Modeling and Simulation (NEAMS) Structural Materials and Chemistry technical area has proposed integrating continuum mechanics codes with those representing chemical phenomena. The vision is to develop a framework for coupling structural behavior with the thermochemistry of a heat transfer fluid (HTF) relevant to both molten salt reactors (MSRs) and light water reactors (LWRs). No existing capability to model the influence of corrosion on mechanical behavior of MSR structural materials exists. All structural alloys currently under consideration for MSR applications contain Cr. Chromium leaching into the molten salt has been identified as a significant problem as its depletion affects the structural integrity of the alloy [1, 2]. Therefore, mechanisms for the Cr leaching phenomenon are proposed and formalisms based on those mechanisms were implemented into the mass transport code Mole, to be described in more detail in Section 3.1. Demonstrations of the leaching phenomenon were benchmarked to experimental data provided by the Molten Salt Reactor campaign.

Leaching and deposition are the dominate physics that drive structural material behavior in HTF loops from a chemistry perspective. Work to date for LWRs has included the impact of CRUD (Chalk River Unidentified Deposits) on reactor physics. The progress made represents a significant step forward in coupling thermochemistry with mass transport and phase transformations modeling. There is an opportunity to leverage and apply the approach to MSRs to simulate the deposition of precipitates in a salt loop. Mole has been calibrated to simulate Cr leaching behavior in an MSR loop, but the capability can be more broadly applied to other HTF systems, for example water in LWRs. Therefore, the two phenomena have been modeled already in some form; this work consolidates leaching and deposition into Mole on the engineering scale to address those important physics that affect structural material behavior in HTF loops.

The focus of this report is a description of the development of an engineering scale transport code. It is part of a larger NEAMS effort for multi-scale modeling of corrosion and chemistry in MSRs. In fiscal year 2020, the five major activities are:

- Development of Mole, an engineering-scale mass transport code applied to leaching of Cr from alloys into molten salts in a flowing loop
- Development of Yellowjacket, a meso-scale mass transport code also applied to Cr diffusion and microstructure evolution in alloys
- Development of a capability to compute molten salt properties using ab-initio techniques
- Thermodynamic modeling and database development of molten salt systems
- Development of a MOOSE qualified Gibbs Energy Minimizer (GEM) for coupling thermochemistry to Mole and Yellowjacket in MOOSE (Multiphysics Object-Oriented Simulation Environment) [3].

2. THE MULTI-SCALE, MULTI-PHYSICS APPROACH FOR CORROSION AND CHEMISTRY MODELING

As discussed, the overarching goal is to develop a multi-scale, multi-physics tool for modeling transport of important components between structural alloys and an HTF and to couple those effects with continuum mechanics codes. Yellowjacket (Section 2.3) provides kinetic information to Mole and both rely on thermodynamic inputs, i.e. phase equilibria and chemical potentials that drive diffusion. Therefore, there is a need for a the Molten Salt Thermodynamic Database (MSTDB) [4] that includes all system components. To interpret the calculations using the MSTDB, a Gibbs Energy Minimizer (GEM) is required. Both of these aspects are discussed later in this section.

Ab-initio techniques are used to generate important properties values such as thermal conductivity, density, and viscosity. Yellowjacket is the link between chemical and structural material behavior. At the mesoscale, it outputs microstructure and compositional profiles that are needed for continuum mechanics simulations.

Common to both the meso- and macro-scale mass transport is the need for validation to experimental benchmark cases. Experiments provide information that give insights into physical mechanisms. An important part of the effort reported here was the interpretation of data derived from corrosion experiments through close coordination with the DOE Molten Salt Reactor Campaign. A detailed description of this work is found in Section 2.4.

2.1 THERMODYNAMIC MODELING AND DATABASE DEVELOPMENT

The current version of MSTDB accommodates 21 elements and models for 54 binary and 26 ternary molten salt solutions along with 14 solid solutions and 140 multicomponent-stoichiometric compounds. The CALculation of PHAsed Diagram (CALPHAD) approach to thermodynamic assessments was used for its development [5]. With CALPHAD, the database can be built upon, or extended, to include more elements as more systems are studied. This will eventually include all the elements that will exist during operation of a molten salt reactor to model the thermochemical behavior with burnup including additives and corrosion products.

It is proposed that in addition to the base salt, and salt fission and activation products the MSTDB should move to include system components for alloys that contact the salt. This is necessary so that phase equilibria and chemical potentials can be coupled to Yellowjacket for predicting microstructure and mass transport in structural materials

2.2 THE GIBBS ENERGY MINIMIZER

The goal is to develop a modern, quality assured GEM for coupling to multi-physics, multi-scale codes in MOOSE [3] that could also be used with other applications outside of the MOOSE framework. It is intended to support modeling and simulation relevant to nuclear fuel systems, i.e. molten salts, oxides, nitrides, alloys etc. The GEM is needed to utilize the MSTDB.

2.3 MESOSCALE MASS TRANSPORT CODE: YELLOWJACKET

Yellowjacket is a mesoscale phase field [6-8] code for mass transport. It is a tool for simulating diffusion processes, microstructural evolution, and pore formation using thermodynamic inputs, specifically chemical potentials and phase equilibria. The aim is for Yellowjacket is to utilize the MOOSE framework to couple to the GEM and Mole [9, 10]. Yellowjacket provides kinetic information for engineering scale modeling in Mole while Mole provides sink terms to Yellowjacket that arise from the dynamic nature of a flowing loop. Mole needs thermal property inputs that must be taken from experimental measurements and/or derived from first principles calculations. Yellowjacket is the coupling point between the chemistry and continuum mechanics codes by providing compositional profiles and microstructure, both of which dominate structural material behavior.

2.4 SEMI-EMPIRICAL CHROMIUM TRANSPORT MODEL DEVELOPMENT

A definitive understanding of the corrosion mechanisms between a multicomponent halide salt (fluorides, chlorides) and multicomponent/ multiphase material is currently missing (Figure 1 shows some of the possible chemical interactions at the salt/alloy interface). This hinders development of physics-based models incorporating thermodynamics of salt/alloy interaction and mass transport mechanisms in the salt. However, there is a need for models to predict metal loss rates of structural materials during exposures in molten salts as a function of time, temperature and alloy composition to model performance, predict lifetimes, and enable selection of suitable materials for successful realization of MSRs. Semi-empirical models were developed considering chemical interactions and transport processes in the alloy based on existing corrosion data for model NiCr alloys exposed in molten chlorides. While these models were developed specifically for chloride salts, they can be applied in the same way to fluoride salts as experimental data becomes available. The approach was to quantify Cr loss from existing corrosion data to generate a description of time and temperature dependence of Cr loss in model NiCr alloys then correlate that to alloy thermodynamics and kinetics. Chemical potentials and mobilities of Cr were then calculated as a function of alloy composition and temperature and a model was developed to predict Cr dissolution rates in molten chloride salts incorporating time, temperature and alloy composition.

Chromium depletion profiles were measured to calculate Cr loss from model NiCr alloys (Ni7Cr, Ni16Cr and Ni24Cr) exposed in binary $KCl\text{-}MgCl_2$ salt mixture at 700°C and 800°C. Figure 2(left) shows the measured Cr profile in Ni24Cr for the 800°C exposure after different times. Taking the variations in salt chemistries in different tests into account, a power law dependence could still be fitted to the calculated Cr loss from the measured profiles at 800°C for the three model alloys. A drop in corrosion rates is expected most likely due to saturation of salt in the capsule.

The models serve as a benchmark for validating depletion test problems for the engineering scale transport code called Mole. The development of the Yellow Jacket discussed above is a companion activity to the work presented here. The semi-empirical models will also be used for benchmarking test problems for that code, as was done for Mole. Follow on work in this area is proposed as follows:

- Correlating measured Cr loss to alloy thermodynamics to describe temperature dependence for corrosion rate constant *k*.
- Simulating corrosion rates in loops by considering the maximum rate (linear portion of Cr loss curve in Figure 2) to model Cr depletion in NiCr alloys.
- Evaluation of applicability of developed correlations for commercial multicomponent alloys by validating with existing experimental data

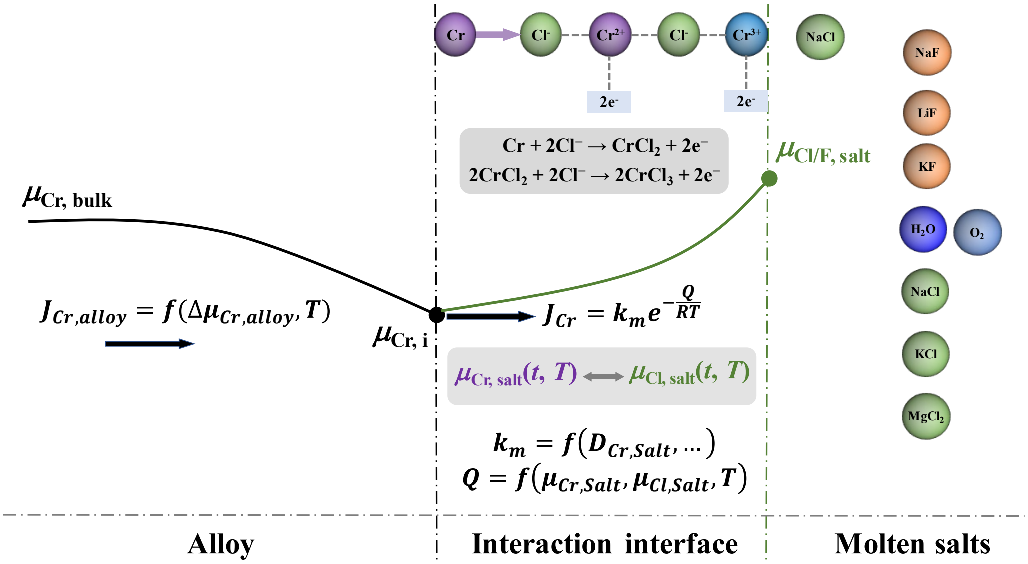

Figure 1 Schematic showing a few potential corrosion reactions, chemical potential gradients and relevant transport processes at a salt/metal interaction interface.

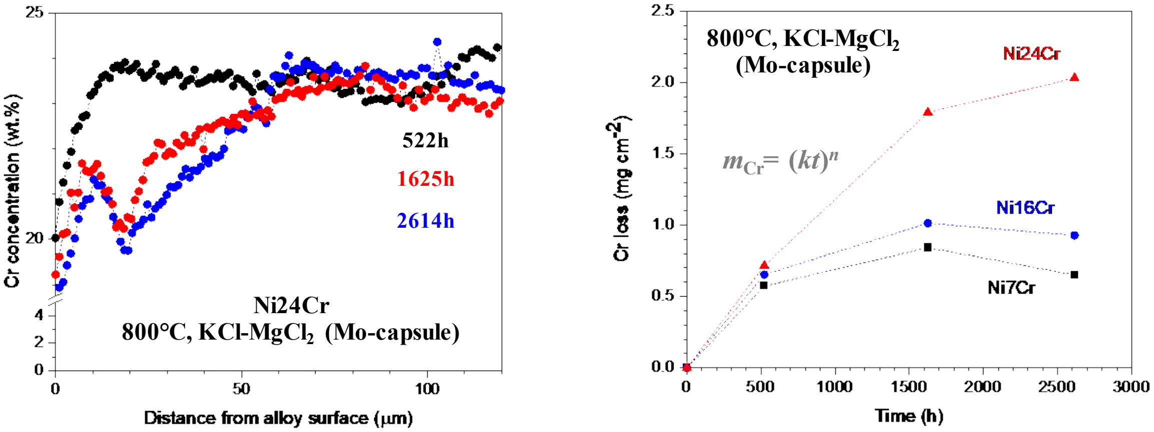

Figure 2 Measured Cr profiles (EDS) in Ni24Cr for different exposure times (left) and Cr loss calculated from measured Cr profiles for Ni7Cr, Ni16Cr and Ni24Cr (right) after exposure at 800°C in KCl-MgCl2 (68:32) salt mixture.

3. ENGINEERING SCALE CODE DEVELOPMENT

3.1 MOLE

Mole is a new code being developed to solve species transport problems for mass accountancy modeling in flowing liquid, i.e. HTF, on the engineering scale. This includes a wide variety of phenomena: movement of species around the primary loop, leaching from system components into a fluid, deposition of species from a fluid onto system components, gas bubble formation, transport of species between gas bubbles and the fluid, and others. The code is built to be flexible, allowing for a wide range of different species to be simulated over a wide variety of time scales.

Mole is built on the MOOSE framework that is a library providing an array of tools for solving finite element method (FEM) problems for a variety of different physics applications. This includes FEM meshing utilities, time-stepping kernels, mesh adaptivity, automatic differentiation, and flexible user inputs to model specific physics. MOOSE is designed to allow development of new physics applications focusing only on the specific physics kernels for their applications without worrying about many details that normally go into the development of a physics code. Additionally, it is also designed for multi-physics coupling, as the name implies, making it straightforward to model physics which have multiple variables that depend on each other.

Mole makes use of the advection solvers that already exist in MOOSE to move species around the loop. Additionally, new features are under development to simplify the tracking of other species and interactions that are of interest for MSR problems. The work presented here specifically makes use of a new kernel called ADArrheniusDeposition, which allows the user to specify a species name and two functions to model the deposition to or leaching from a system component. This kernel takes the following form:

$$R(T) = A\, e^{-\frac{B}{T}},$$

where T is the temperature variable and A and B are the user-specified constants.

3.2 INTEGRATION WITH NEAMS WORKBENCH

One advantage of working building Mole on the MOOSE framework is that this readily allows for integration with the NEAMS Workbench[11]. The Workbench provides a number of valuable features to support development and use of NEAMS tools, including real-time input validation for a variety of input files (MOOSE-based inputs being one of them), local and remote job launch with the required controls for job submissions systems such as PBS, and built-in post-processing for certain output files. Because Mole is built on MOOSE, the Workbench already has the capability to query the Mole code for valid input syntax so that it can provide dynamic input validation, even for a brand new code that had not been previously tested with the Workbench.

The calculations presented in the coming sections were completed using the NEAMS Workbench. Screenshots are included showing the file navigation and input validation capabilities. After setting up and validating these inputs, the jobs were run on remote clusters using the Workbench job launch capability. Most significantly, the Dakota sensitivity study presented toward the end of Section 3 was performed and postprocessed using the Workbench. This task would have been significantly more difficult without the integrated capabilities of the Workbench.

3.3 CHROMIUM LEACHING EXPERIMENT BENCHMARKING

To validate the capability, a model was generated from experimental data. In the experiment, nickel-chromium (Ni-Cr) alloys were exposed to a molten salt at 800 C for approximately 2700 hours. Three different alloys were tested based on amount of chromium in the alloy, by weight percent (wt%): 7 wt%, 16 wt%, and 24 wt%. Curves were fit to the data as function of Cr wt% and temperature using a power law:

$$
\begin{gathered}
m_L(t, W_{Cr}, T) = (kt)^{\frac{1}{2}}, \\
k = \frac{k_0 W_{Cr}}{7} e^{-\frac{Q}{RT}}, \\
k_0 = 3.45 \times 10^5 \, mg^2 \, cm^{-4} \, h^{-1}, \\
Q = 180 \, kJ \, mol^{-1}, \\
R = 8.314 \times 10^{-3} \, kJ \, mol^{-1} \, K^{-1},
\end{gathered} \tag{1}
$$

where t is the elapsed time (hours) and W_Cr is the Cr wt% (7, 16, or 24 for this experiment).

3.4 EXPERIMENT MODEL IN MOLE

3.4.1 Experimental data form

To fit the form of the Arrhenius rate equation implemented in Mole, this function m_L (t,T) was assumed to be the analytic solution for a differential equation describing the rate of chromium depletion from the alloy:

$$\frac{dm_L}{dt} = A(t, W_{Cr}) e^{-\frac{B}{T}}.$$

Taking the derivative gives the necessary coefficients required by Mole:

$$
\begin{gathered}
A(t, W_{Cr}) = \frac{1}{2}\sqrt{\frac{k_0 W_{Cr}}{7t}}, \\
B = \frac{Q}{2R}.
\end{gathered}
$$

These coefficients were directly plugged into the Arrhenius rate material in Mole (as shown in Figure 3), which feeds into a solver kernel used in the MOOSE FEM solve. An input file snippet below shows the definition of the coefficients and other functions that feed into them:

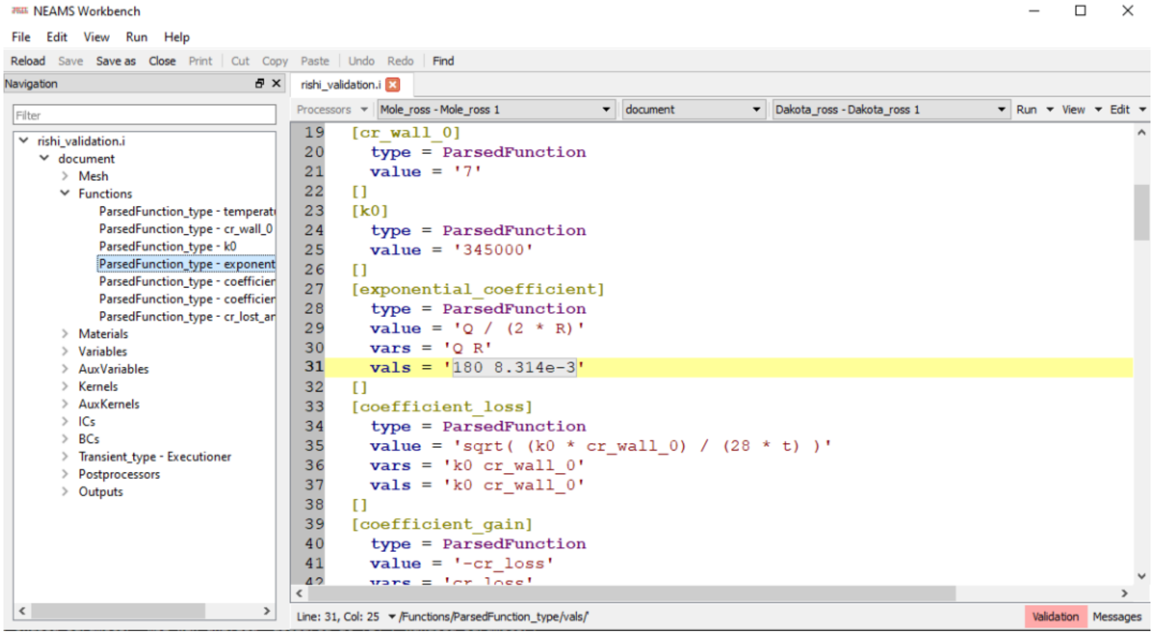

```
[cr_wall_0]
  type = ParsedFunction
  value = '7'
[]
[k0]
  type = ParsedFunction
  value = '345000'
[]
[exponential_coefficient]
  type = ParsedFunction
  value = 'Q / (2 * R)'
  vars = 'Q R'
  vals = '180 8.314e-3'
[]
[coefficient_loss]
  type = ParsedFunction
  value = 'sqrt( (k0 * cr_wall_0) / (28 * t) )'
  vars = 'k0 cr_wall_0'
  vals = 'k0 cr_wall_0'
[]
[coefficient_gain]
  type = ParsedFunction
  value = '-cr_loss'
  vars = 'cr_loss'
```

Figure 3: User inputs to define the Arrhenius leaching rates in Mole using NEAMS Workbench [12, 13]

3.4.2 Mesh and variable models

The salt loop has a total length of approximately 263 cm. This was modeled in Mole as a 1D line with periodic boundaries at the ends of the line. 2500 mesh elements were used to discretize the line. The “cr_wall” and “cr_liquid” variables shown in Figure 4 are the chromium in the “wall” (or alloy sample, in this case) and liquid (the molten salt), respectively. It was assumed that all chromium that leached from the alloy remained in the salt, so looking at the amount of chromium in the liquid is consistent when comparing to the experimentally derived m_L function.

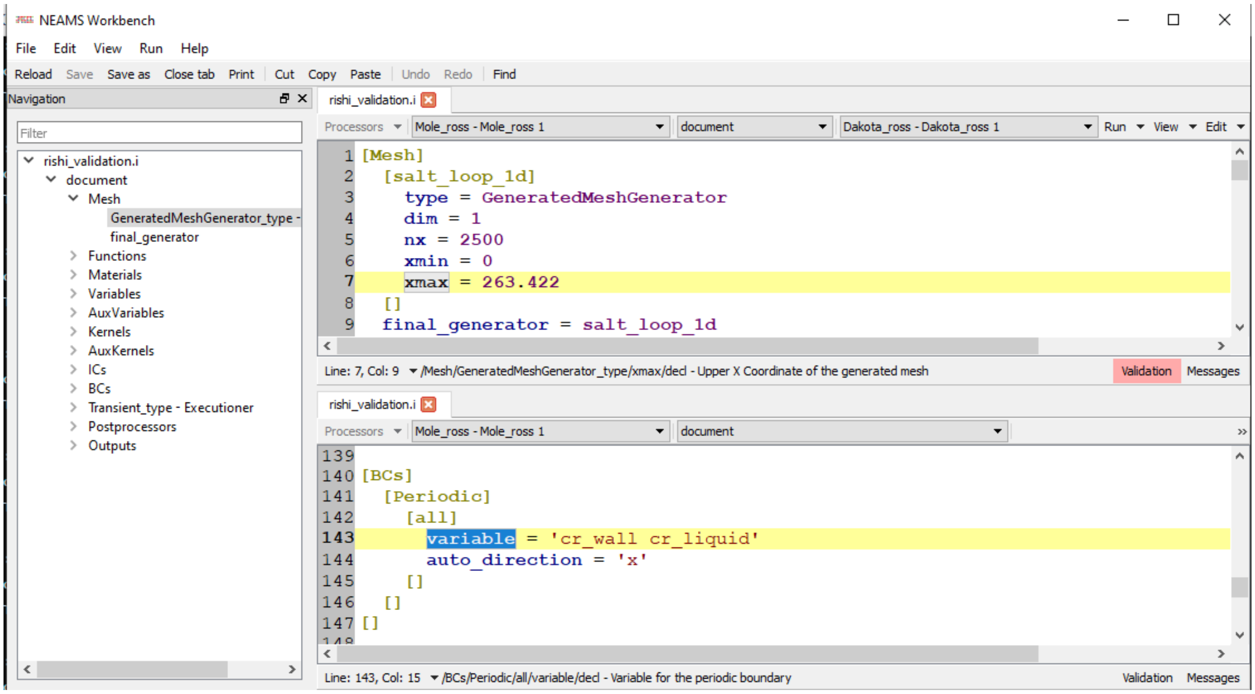

```
[Mesh]
  [salt_loop_1d]
    type = GeneratedMeshGenerator
    dim = 1
    nx = 2500
    xmin = 0
    xmax = 263.422
  []
  final_generator = salt_loop_1d
```

Line: 7, Col: 9 /Mesh/GeneratedMeshGenerator_type/xmax/decl - Upper X Coordinate of the generated mesh

```

[BCs]
  [Periodic]
    [all]
      variable = 'cr_wall cr_liquid'
      auto_direction = 'x'
    []
  []
[]
```

Line: 143, Col: 15 /BCs/Periodic/all/variable/decl - Variable for the periodic boundary

Figure 4: User inputs to define the mesh and boundary conditions in Mole using NEAMS Workbench

3.5 PHYSICS KERNELS

Typically, Mole would apply convection kernels to this problem. However, because the experimental models are integral quantities for total loss of chromium from the alloy, no convection effects are accounted for in the model. Thus, the only kernels required are for the Arrhenius loss rate and the time derivative. Note that the “ADArrheniusDeposition” kernel can be used for either material deposition or leaching, depending on the presence of a negative sign in the input parameters. The kernel inputs are shown in Figure 5.

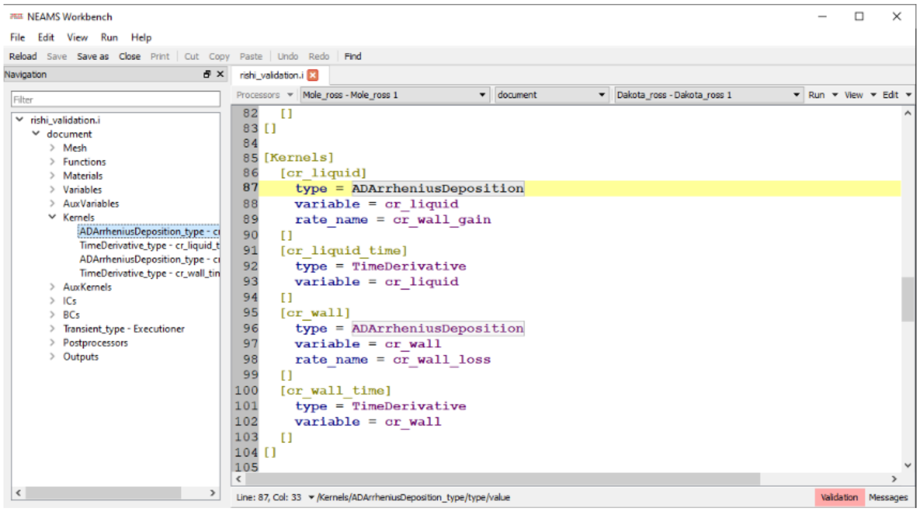

```
  []
[]

[Kernels]
  [cr_liquid]
    type = ADArrheniusDeposition
    variable = cr_liquid
    rate_name = cr_wall_gain
  []
  [cr_liquid_time]
    type = TimeDerivative
    variable = cr_liquid
  []
  [cr_wall]
    type = ADArrheniusDeposition
    variable = cr_wall
    rate_name = cr_wall_loss
  []
  [cr_wall_time]
    type = TimeDerivative
    variable = cr_wall
  []
[]
```

Figure 5: User inputs to define the solver kernels in Mole using NEAMS Workbench

Additionally, an "auxiliary kernel" was set up with the m_L function. Auxiliary kernels in MOOSE calculate variables that are not actually part of the equation being solved, but are of interest to the user and can be calculated using solution variables. In this case, the auxiliary variable "cr_lost_analytic" was compared to the solution variable "cr_l" to determine the accuracy of Mole's predictions. The material inputs and analytic solution setup are shown in Figure 6.

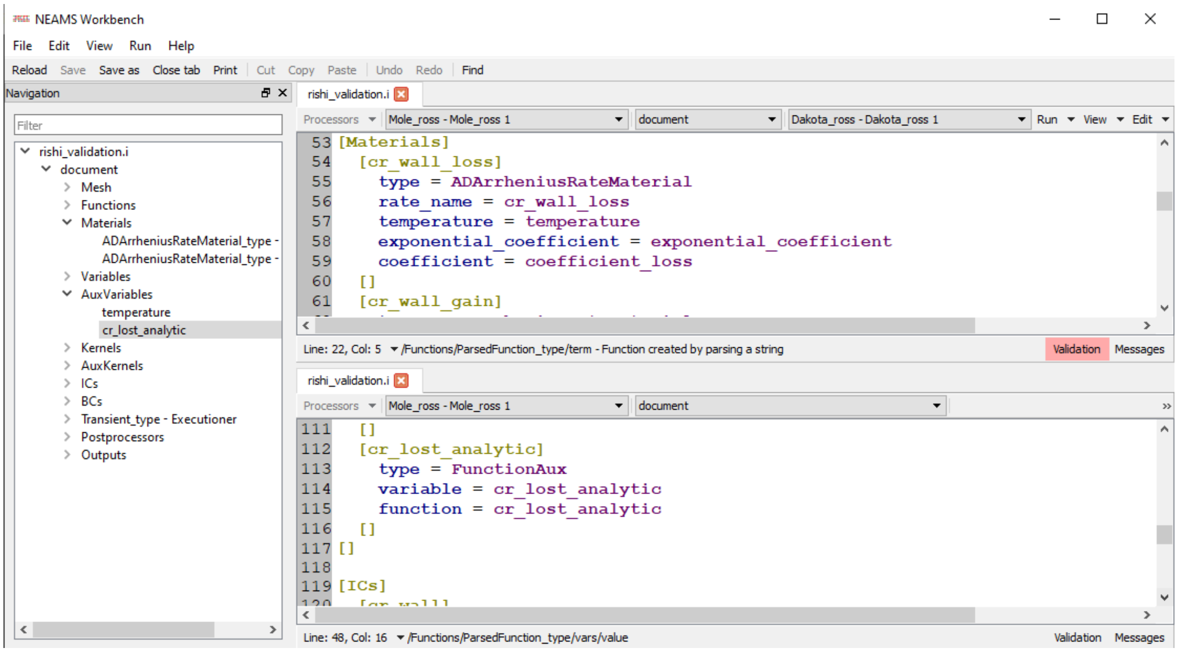

```
[Materials]
  [cr_wall_loss]
    type = ADArrheniusRateMaterial
    rate_name = cr_wall_loss
    temperature = temperature
    exponential_coefficient = exponential_coefficient
    coefficient = coefficient_loss
  []
  [cr_wall_gain]
```

```
  []
  [cr_lost_analytic]
    type = FunctionAux
    variable = cr_lost_analytic
    function = cr_lost_analytic
  []
[]

[ICs]
```

Figure 6: User inputs to define the Arrhenius rate material and analytic solution in Mole using NEAMS Workbench

3.6 RESULTS

The results of the Mole validation work are presented here. For each of the 3 alloys, a set of solutions and errors are presented. For the solutions, the analytic solution (developed model m_L (t,W_Cr,T)) is presented along with Mole's solution using time-steps of 1, 10, 100, or 1000 hours. In the case of 1000 hours, the final time-step is truncated to 700 hours to match the end of the experiment. A separate plot is then presented showing the relative error of the Mole solution defined as

$$\frac{m_M - m_L}{m_L},$$

where m_M is the solution predicted by Mole.

The results are shown in Figure 7 (7 wt%), Figure 8 (16 wt%), and Figure 9 (24 wt%), along with relative errors for each calculation, with relative error being defined as the difference between the mole solution and experimental model divided by the value of the experimental model. A Crank-Nicolson time-stepping procedure was applied to the calculation, which has second-order convergence properties. Clearly the errors are unacceptably large for the coarser time-steps, but with finer time-steps, the relative differences between Mole and the experimental model are quite small, especially toward the end of the simulation. The error in the time-stepping method is proportional to the derivatives of the solution, so the errors shrink at later times because the solution changes more gradually.

Additionally, the relative error as a function of time for each of the 3 alloys is identical. Again, this is because the error of the time-stepping method is a function of the derivative of the analytic solution and some constants. The difference in the errors between 2 alloys for the same time-step size will only be a function of the constants that are alloy dependent. By taking the relative error, those constants cancel out, giving the same relative error curves for all 3 alloys.

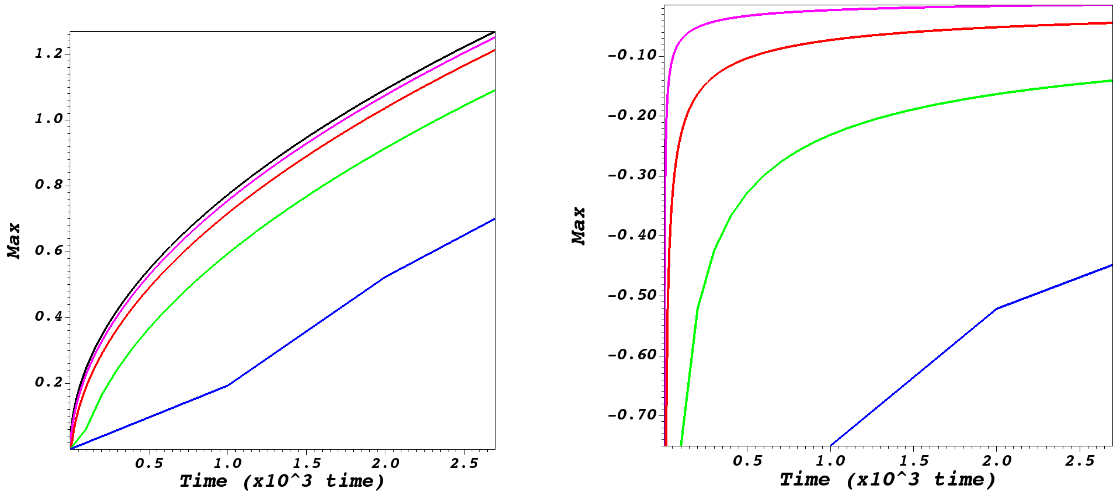

Figure 7: The results (left) and relative error (right) of the Mole calculations for a Ni-Cr alloy with 7 wt% Cr; results shown for experimental model (black) and time-step sizes of 1000 hours (blue), 100 hours (green), 10 hours (red), and 1 hour (magenta). The units are hours for the time axis and mg/cm^2 for the vertical axis.

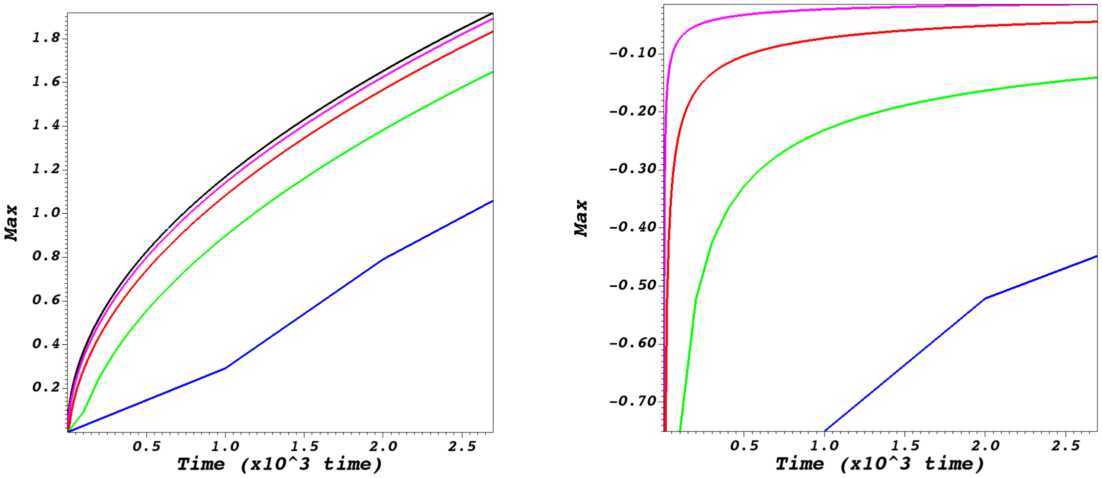

Figure 8: The results (left) and relative error (right) of the Mole calculations for a Ni-Cr alloy with 16 wt% Cr; results shown for experimental model (black) and time-step sizes of 1000 hours (blue), 100 hours (green), 10 hours (red), and 1 hour (magenta). The units are hours for the time axis and mg/cm² for the vertical axis.

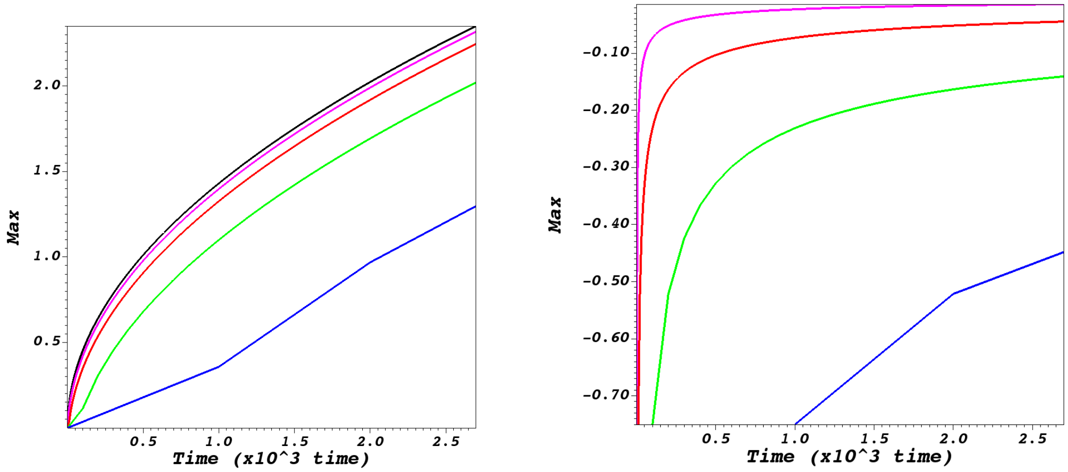

Figure 9: The results (left) and relative error (right) of the Mole calculations for a Ni-Cr alloy with 24 wt% Cr; results shown for experimental model (black) and time-step sizes of 1000 hours (blue), 100 hours (green), 10 hours (red), and 1 hour (magenta) The units are hours for the time axis and mg/cm² for the vertical axis..

These results show that if the experimental data is in the proper form and a sufficiently refined time-step is used, Mole is fully capable of modeling chemistry problems such as chromium leaching from an alloy. Moving forward, work will be done to apply this code to a wider variety of chemistry problems related to MSR modeling and simulation.

3.7 SAMPLE LOOP WITH LEACHING AND DEPOSITION

In addition to experimental validation, the current capabilities of Mole to simulate the primary loop of an MSR or other similar molten salt systems can be demonstrated using a simplified MSR loop model. This model is a 1D model of a primary loop. The length is 400 cm long. To model a heater, there is a linear temperature rise from 700 C to 800 C from 0 cm to 150 cm; likewise, to model a heat exchanger, there is a temperature decrease from 800 C back to 700 C from 200 cm to 250 cm. Leaching of chromium into the salt is allowed everywhere in the loop except the heat exchanger, and deposition of chromium from the salt onto the wall is allowed only in the heat exchanger. The leaching rates are the same functions of temperature as used in the experimental validation in previous sections. For the deposition rates, an Arrhenius function was used again. However, in this case, the coefficients were simply selected to cause a significant amount of deposition over the time interval examined:

$$\frac{dm_{L\to W}}{dt}(T) = A\,e^{-\frac{B}{T}}$$

$$A = 0.01$$

$$B = 10.0$$

The model was simulated for 2,700 hours as with the experimental validation model. Time-steps of 1 hour were used.

In addition to adding deposition, advection was also added to carry the chromium leaching from the heater to the heat exchanger. A constant flowrate of 10 cm/s was used everywhere in the model. This advection makes the model more realistic, as well as demonstrating the capabilities of mole. The inputs for the velocity variables and kernels are shown below in Figure 10.

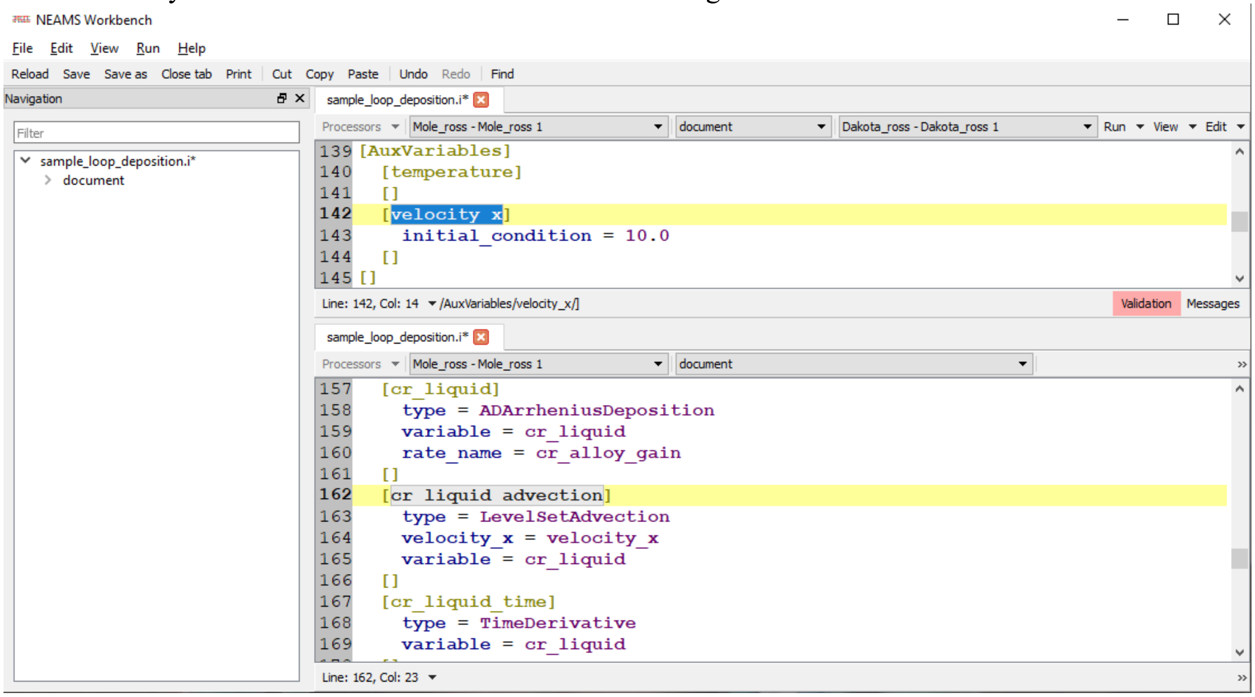

```
[AuxVariables]
  [temperature]
  []
  [velocity_x]
    initial_condition = 10.0
  []
[]
```

```
  [cr_liquid]
    type = ADArrheniusDeposition
    variable = cr_liquid
    rate_name = cr_alloy_gain
  []
  [cr_liquid_advection]
    type = LevelSetAdvection
    velocity_x = velocity_x
    variable = cr_liquid
  []
  [cr_liquid_time]
    type = TimeDerivative
    variable = cr_liquid
```

Figure 10: Velocity variable and kernel definitions for sample loop model in Mole

The figures below show the temperature distribution for the model specified in the input (Figure 11), the resulting distribution of chromium in the molten salt (Figure 12), and the amount of chromium deposited from the salt onto the heat exchanger walls (Figure 13). The distribution for the liquid peaks after the heater and has its minimum after the heat exchanger, but with a relatively small difference between the two. These maximum and minimum locations are expected since the chromium in the salt builds up in the heater and deposits out of the salt in the heat exchanger. The small difference between the minimum and maximum is due to the flow of the salt. The deposition rates in the heat exchanger are around 1-2% per second (depending on temperature), but the salt is flowing at 10 cm/s through a heat exchanger that is only 50 cm long. Thus, over time the chromium that has leached into the salt becomes fairly well mixed, explaining the small difference between the minimum and maximum amounts in the liquid at the end of the simulation.

In Figure 13, the primary loop is blacked out except for the heat exchanger region to emphasize that deposition is only allowed to occur in the heat exchanger portion of the loop. The deposited chromium is zero everywhere else. The deposited chromium follows the expected trends in the heat exchanger, just as the dissolved chromium in the liquid did throughout the loop. The deposition rates are defined relative to the concentration in the salt, so as the salt flows through the heat exchanger and cools, there is less chromium to deposit onto the heat exchanger wall. Thus, the peak chromium deposits are at the very beginning of the heat exchanger and steadily drop off until the end of the heat exchanger.

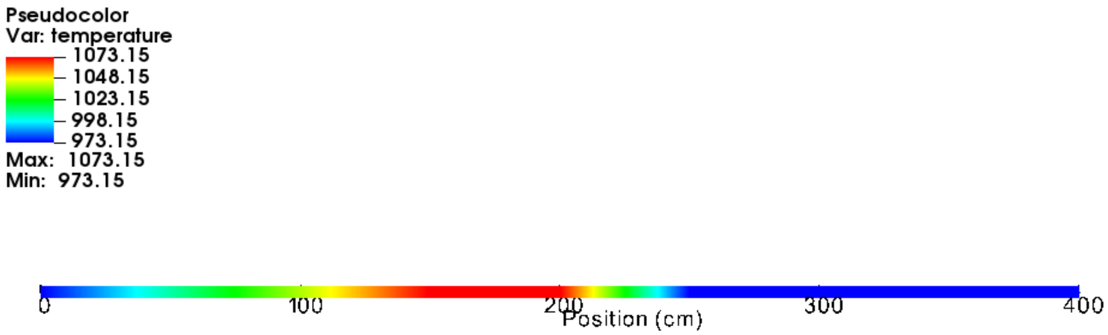

Figure 11: Temperature distribution (K) for sample loop model in Mole

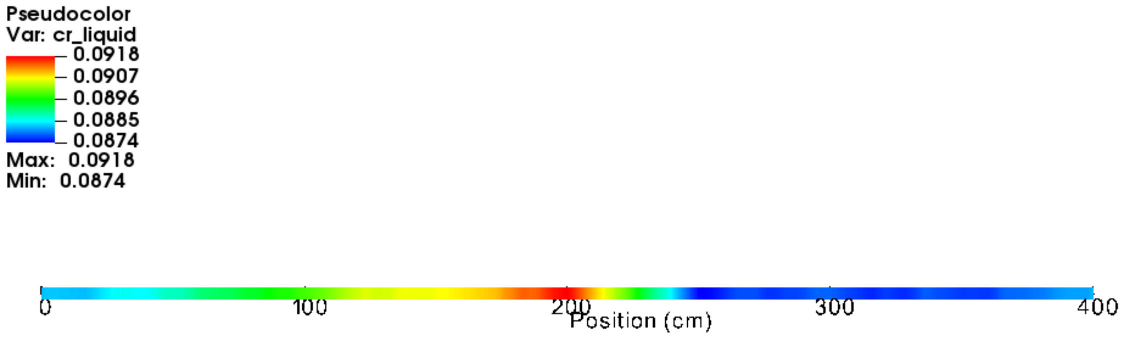

Figure 12: Mass distribution (mg) of chromium dissolved in the molten salt for sample loop model in Mole after 2700 simulation hours

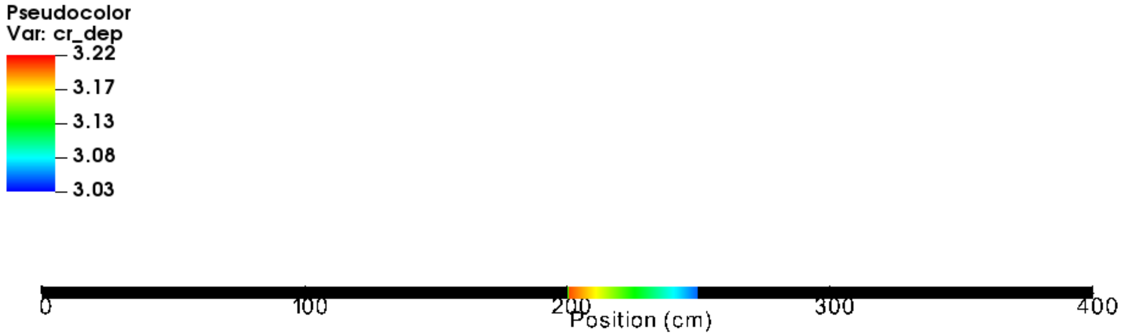

Figure 13: Mass distribution (mg) of chromium deposited on the heat exchanger walls for sample loop model in Mole after 2700 simulation hours

Finally, Figure 14 shows the maximum amount of chromium deposited in the heat exchanger in units of mg as function of time. In this case, this is simply the amount of deposited chromium at 200 cm since that is always the point that had the most deposition. However, this shows that Mole can capture the change in solution as a function of time.

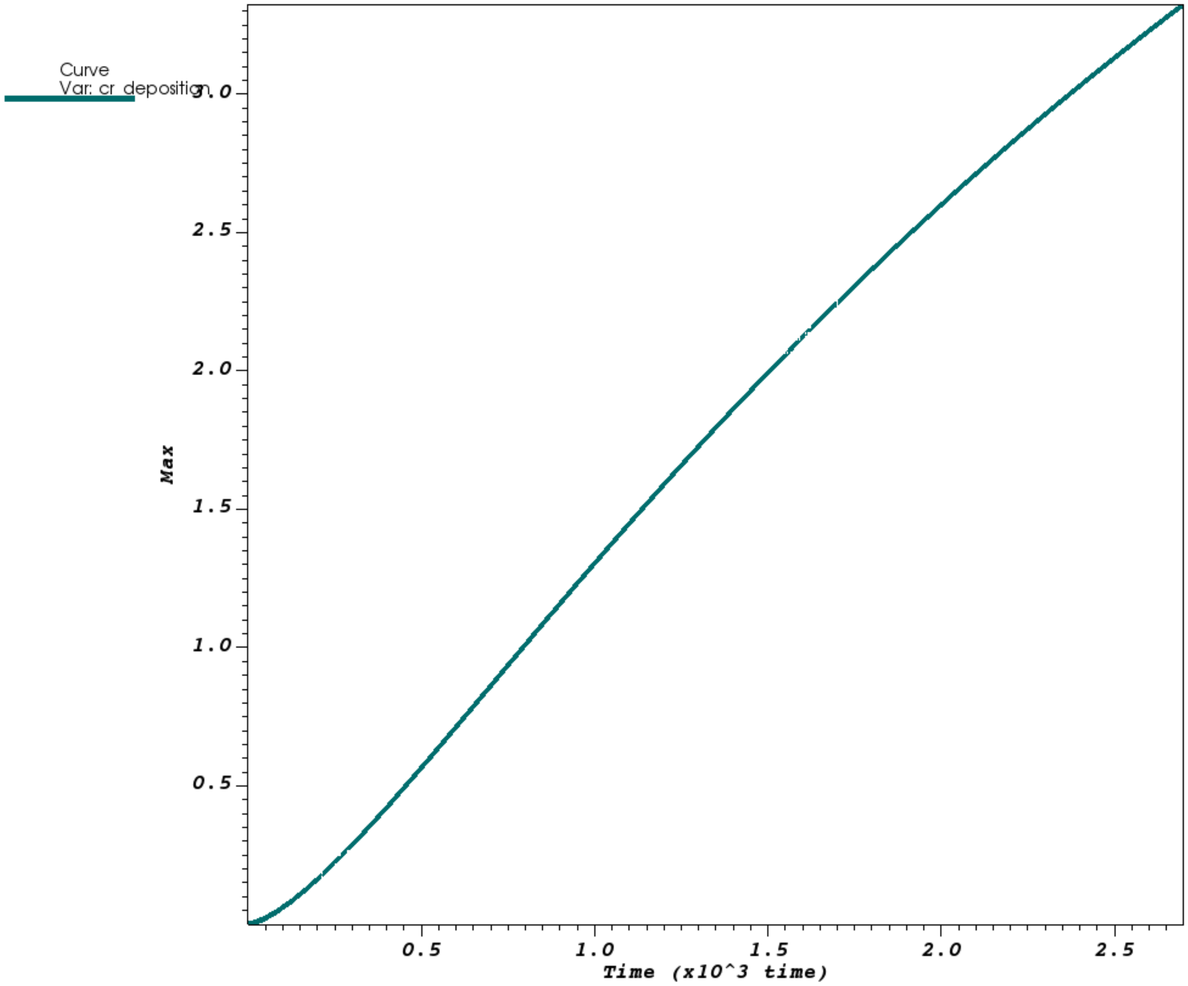

Figure 14: Maximum chromium deposition (mg) in the heat exchanger as a function of time (h)

3.8 SAMPLE LOOP SENSITIVITY STUDY USING DAKOTA

One of the previously mentioned features of workbench was the ability to use Dakota to perform uncertainty quantification and sensitivity studies. To demonstrate this, a sensitivity study was done using Dakota and Mole on the sample loop problem from the previous section. Dakota allows the user to "template" portions of an input to another code, in this case Mole, and then provide distribution descriptions from which to sample that input. A portion of the Dakota input is shown below, followed by one of the sample loop templates. The calculations below will sample from a Gaussian distribution for each of four templated input parameters. The mean of the distribution will be the values used in previous sections (derived from experimental model for leaching, or selected values for deposition). The values that were templated for these studies were the leaching and deposition pre-exponential coefficients (k_0 in the experimental leaching model and A in deposition model) and the leaching and deposition activation energies (Q in the experimental leaching model and B in the deposition model). This input templating is demonstrated in Figure 15.

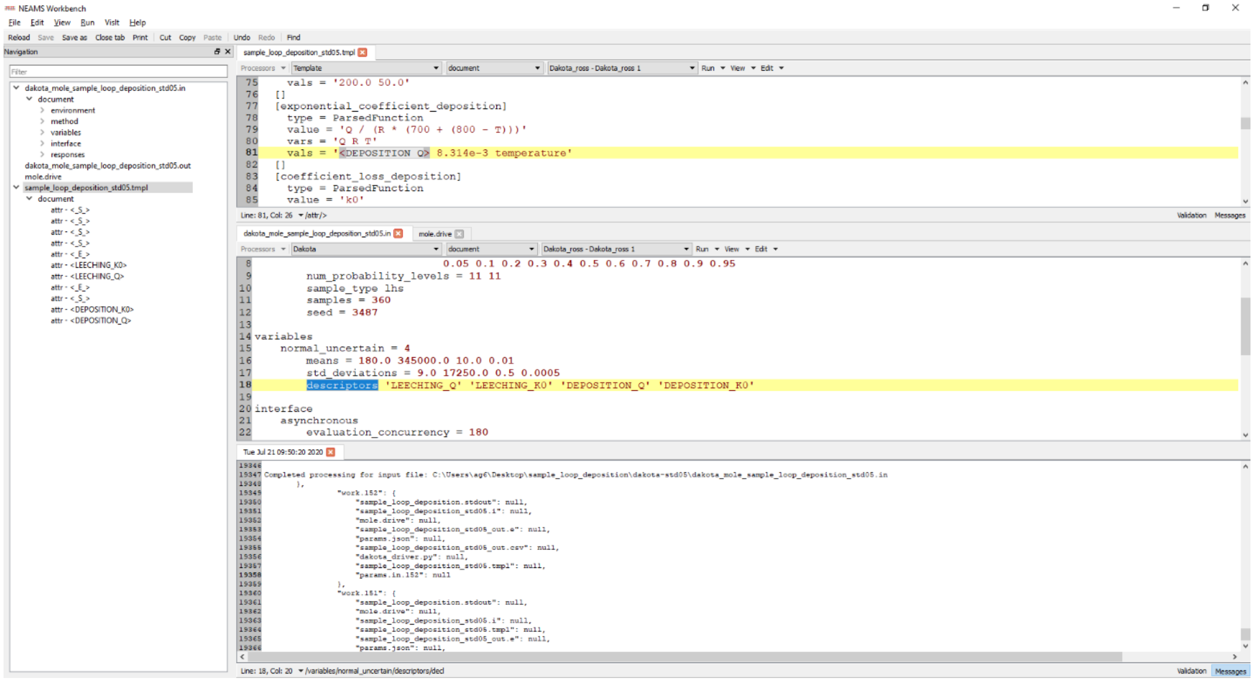

```
    vals = '200.0 50.0'
  []
  [exponential_coefficient_deposition]
    type = ParsedFunction
    value = 'Q / (R * (700 + (800 - T)))'
    vars = 'Q R T'
    vals = '<DEPOSITION_Q> 8.314e-3 temperature'
  []
  [coefficient_loss_deposition]
    type = ParsedFunction
    value = 'k0'
```

```
                                  0.05 0.1 0.2 0.3 0.4 0.5 0.6 0.7 0.8 0.9 0.95
        num_probability_levels = 11 11
        sample_type lhs
        samples = 360
        seed = 3487

variables
    normal_uncertain = 4
        means = 180.0 345000.0 10.0 0.01
        std_deviations = 9.0 17250.0 0.5 0.0005
        descriptors 'LEECHING_Q' 'LEECHING_K0' 'DEPOSITION_Q' 'DEPOSITION_K0'

interface
    asynchronous
        evaluation_concurrency = 180
```

```

Completed processing for input file: C:\Users\ag6\Desktop\sample_loop_deposition\dakota-std05\dakota_mole_sample_loop_deposition_std05.in
        },
                "work.152": {
                    "sample_loop_deposition.stdout": null,
                    "sample_loop_deposition_std05.i": null,
                    "mole.drive": null,
                    "sample_loop_deposition_std05_out.e": null,
                    "params.json": null,
                    "sample_loop_deposition_std05_out.csv": null,
                    "dakota_driver.py": null,
                    "sample_loop_deposition_std05.tmpl": null,
                    "params.in.152": null
                },
                "work.151": {
                    "sample_loop_deposition.stdout": null,
                    "mole.drive": null,
                    "sample_loop_deposition_std05.i": null,
                    "sample_loop_deposition_std05.tmpl": null,
                    "sample_loop_deposition_std05_out.e": null,
                    "params.json": null,
```

Figure 15 Remote execution of Dakota sensitivity calculations for Mole using the NEAMS Workbench

Two sets of studies were done: one with 5% standard deviation (shown in the inputs below) and one with 10% standard deviation. 360 total calculations were run for each case, sampling all 4 of the templated variables at a time. Dakota has a "concurrent evaluation" capability, which allows it to drive multiple calculations simultaneously. Thus, the 360 calculations for each sensitivity study were done in 10 batches of 36 concurrent evaluations on the remote cluster. The results were then copied back to the local machine for postprocessing. A time-step size of 100 hours was used for these calculations.

To postprocess the results, the NEAMS Workbench has built-in postprocessing and visualization capabilities, shown in Figure 16. For these calculations specifically, the partial and simple correlation matrixes can be processed from the Dakota output and visualized using Visit.

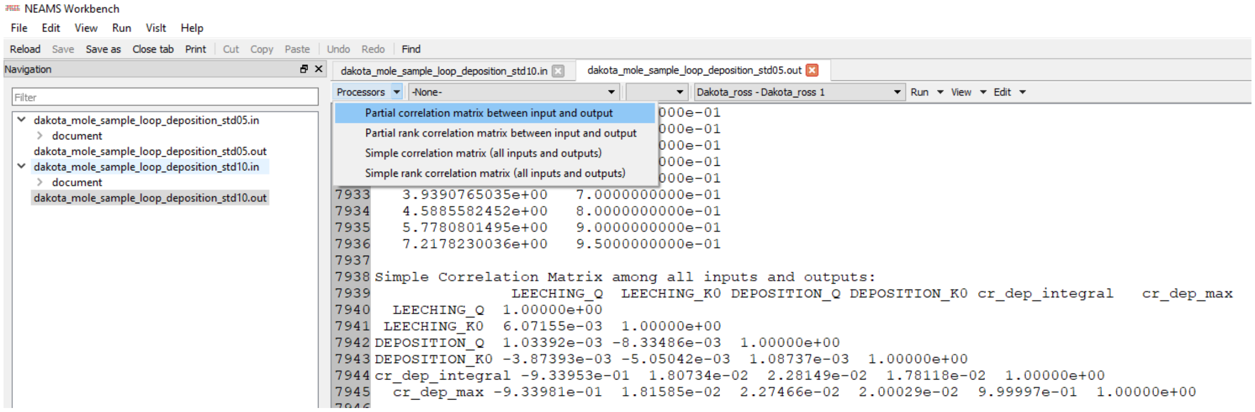

```
                    000e-01
                    000e-01
                    000e-01
                    000e-01
                    000e-01
   3.9390765035e+00   7.0000000000e-01
   4.5885582452e+00   8.0000000000e-01
   5.7780801495e+00   9.0000000000e-01
   7.2178230036e+00   9.5000000000e-01

Simple Correlation Matrix among all inputs and outputs:
               LEECHING_Q  LEECHING_K0 DEPOSITION_Q DEPOSITION_K0 cr_dep_integral   cr_dep_max
  LEECHING_Q  1.00000e+00
 LEECHING_K0  6.07155e-03  1.00000e+00
DEPOSITION_Q  1.03392e-03 -8.33486e-03  1.00000e+00
DEPOSITION_K0 -3.87393e-03 -5.05042e-03  1.08737e-03  1.00000e+00
cr_dep_integral -9.33953e-01  1.80734e-02  2.28149e-02  1.78118e-02  1.00000e+00
  cr_dep_max -9.33981e-01  1.81585e-02  2.27466e-02  2.00029e-02  9.99997e-01  1.00000e+00
```

Figure 16: Screenshot of postprocessing options for Dakota output in NEAMS Workbench

Figure 17 shows the partial correlation matrix for the 5% case. The two output quantities of interest are the maximum chromium deposition and the integral (over the length of the heat exchanger) of the chromium deposition. Since these are essentially different measurements of the same quantity, the correlations between the inputs and each output are essentially the same. However, this demonstrates how multiple input and multiple outputs can be correlated with each other. The most strongly correlated input is the leaching activation energy. This value is highly influential to the amount of chromium that leaches into the salt, and thus also to the amount that is available to deposit in the heat exchanger. The other 3 inputs have comparatively small effects on the deposition, at least over the range sampled in this problem.

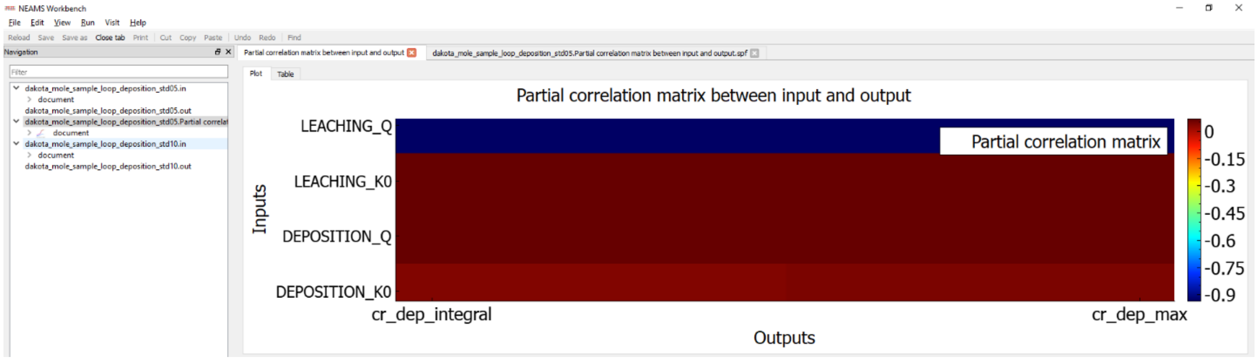

Figure 17: Partial correlation matrix between inputs and outputs for sample loop in Mole using a 5% standard deviation

Figure 18 shows the same partial correlation matrix as before, except this time sampled using a 10% standard deviation instead of 5%. For this case, the broader distributions did not have any discernible impact on the correlations, with the leaching activation energy still being the dominant factor. Additionally, the full correlation matrix between all inputs and outputs is shown in Figure 19. This does not reveal anything important that was not clear from the partial correlation matrix, but could be useful in other more detailed analyses.

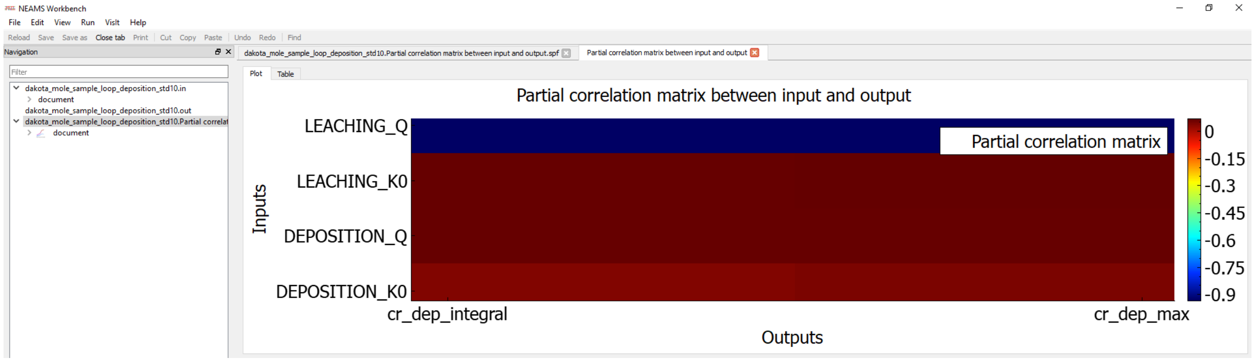

Figure 18: Partial correlation matrix between inputs and outputs for sample loop in Mole using a 10% standard deviation

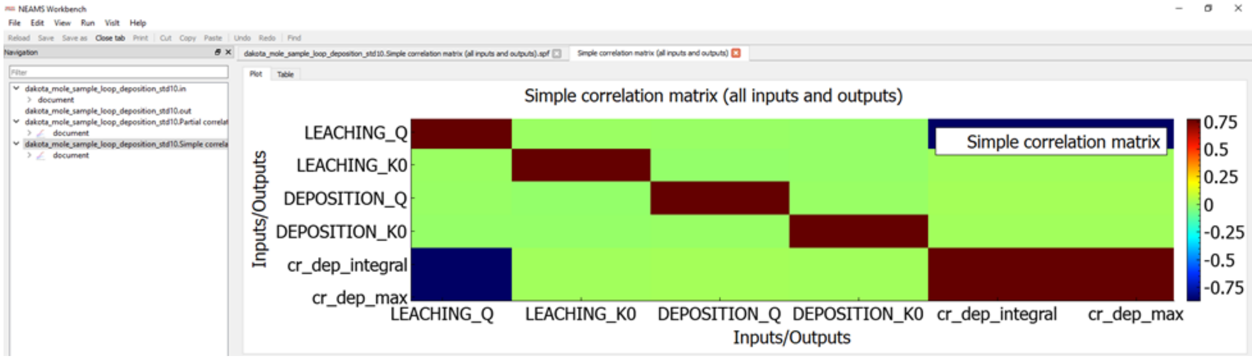

Figure 19: Simple correlation matrix between all inputs and all outputs for sample loop in Mole using a 10% standard deviation.

4. CONCLUSIONS AND FUTURE WORK

This report has summarized the current status of a new engineering scale molten salt chemistry and corrosion code Mole. The code takes advantage of much pre-existing work in finite element meshing, linear and non-linear solvers, and multiphysics coupling by using the MOOSE framework. Experimental measurements of chromium depletion from nickel-chromium alloys was used to develop a model against which to test Mole. Initial results demonstrate that with sufficiently refined time-steps, Mole is capable of accurately resolving the model developed from the experimental data.

Additionally, other capabilities of Mole were exercised using a simple salt loop model composed of a heater and a heat exchanger. Calculations with this model show the ability of Mole to capture not only chromium leaching, but also advection of the dissolved chromium around the loop and deposition of the chromium onto other component surfaces. Integration of Mole with the NEAMS workbench was also demonstrated successfully, along with driving Dakota sensitivity studies on Mole input parameters through the Workbench.

Some initial experimental validation and other demonstrations with Mole have been successful. Moving forward, efforts in Mole development should focus on two primary areas: transport models and multiphysics coupling. It is proposed that transport model development focus on extending the capabilities of Mole beyond simply leaching, advection, and deposition to other important phenomena. Multiphysics development should focus on coupling Mole with other codes that can provide some of the inputs that were user-specified for this report. For example, coupling to a systems code can provide velocity and temperature distributions for the salt loop, and coupling to a code such as Yellowjacket can provide more dynamic, detailed rate constants for corrosion calculations. Continued development of Mole in these two areas can provide a flexible, robust molten salt modeling tool to analyze chemistry and corrosion phenomena, mass accountancy, and feedback effects for other physics of interest.

5. REFERENCES

[1] W. Ding, J. Gomez-Vidal, A. Bonk, T. Bauer, *Sol. Energy Mater.*, 199 (2019) 8-15.
[2] L. C. Olson, J. W. Ambrosek, K. Sridharan, M. H. Anderson, T. R. Allen, *J. Fluorine Chem.*, 130 (1) (2009) 67-73.
[3] C. J. Permann, D. R. Gaston, D. Andrš, R. W. Carlsen, F. Kong, A. D. Lindsay, J. M. Miller, J. W. Peterson, A. E. Slaughter, R. H. Stogner, *SoftwareX*, 11 (2020) 100430.
[4] T. M. Besmann, J. Ard, S. Utlak, J. W. Mcmurray, R. A. Lefebvre, Status of the salt thermochemical database, Oak Ridge National Lab.(ORNL), Oak Ridge, TN (United States), (2019)
[5] CALPHAD, http://www.thermocalc.com/academia/researchers/calphad/
[6] L.-Q. Chen, *Annual review of materials research*, 32 (1) (2002) 113-40.
[7] N. Moelans, B. Blanpain, P. Wollants, *CALPHAD*, 32 (2) (2008) 268-94.
[8] M. R. Tonks, L. K. Aagesen, *Annual Review of Materials Research*, 49 (2019) 79-102.
[9] D. Schwen, L. K. Aagesen, J. W. Peterson, M. R. Tonks, *Comput. Mater. Sci.*, 132 (2017) 36-45.
[10] M. R. Tonks, D. Gaston, P. C. Millett, D. Andrs, P. Talbot, *Comput. Mater. Sci.*, 51 (1) (2012) 20-9.
[11] B. M. Adams, W. J. Bohnhoff, K. R. Dalbey, Ebeida, M.S., J. P. Eddy, M. S. Eldred, G. Geraci, R. W. Hooper, P. D. Hough, K. T. Hu, J. D. Jakeman, M. Khalil, K. A. Maupin, J. A. Monschke, E. M. Ridgway, A. A. Rushdi, J. A. Stephens, L. P. Swiler, D. M. Vigil, T. M. Wildey, J. G. Winokur, Dakota, A Multilevel Parallel Object-Oriented Framework for Design Optimization, Parameter Estimation, Uncertainty Quantification, and Sensitivity Analysis: Version 6.11 User's Manual
Sandia National Laboratory, (2019)
[12] R. A. Lefebvre, B. R. Langley, L. P. Miller, M.-O. G. Delchini, M. Baird, J. P. Lefebvre, NEAMS Workbench Status and Capabilities, Oak Ridge National Lab.(ORNL), Oak Ridge, TN, (2019)
[13] R. A. Lefebvre, B. R. Langley, A. B. Thompson, M3ms-16or0401086–report on NEAMS workbench support for moose applications, Technical report, Oak Ridge National Lab.(ORNL), Oak Ridge, TN, (2016)